J Supercond Nov Magn (2015) 28:579–583
DOI 10.1007/s10948-014-2717-7

ORIGINAL PAPER

Dynamic Inductance in Saturated Cores Fault Current Limiters

Y. Nikulshin · Y. Wolfus · A. Friedman · Y. Yeshurun

Received: 10 June 2014 / Accepted: 18 August 2014 / Published online: 21 September 2014

Abstract The saturated cores Fault Current Limiter (FCL) is one of the leading candidates for providing a commercial robust solution to the fault current problem. Basically, the saturated cores FCL offers low impedance during normal grid operation due to its saturated cores state and high impedance in fault events due to cores desaturation. We developed a method to obtain the nonlinear inductance curve $L(I)$ of the saturated cores FCL from which we show that the dynamic inductance component, dL/dt, contributes significantly to the FCL limiting capabilities. Specifically, we show that in some parts of the AC cycle, the dynamic inductance term dominates over the static inductance in contributing to the voltage drop across the device. We conclude that the design of saturated cores FCL should consider the dynamic inductance and calculate its contribution to the FCL voltage to benefit from better device performances.

Keywords Fault current limiter · Magnetic cores · Superconducting devices · Smart grids · High-power applications

1 Introduction

Recent successful installations of saturated cores Fault Current Limiter (FCL) devices have demonstrated the potential of the saturated cores FCL for providing commercial solution to fault currents in distribution and transmission grids. In 2007, InnoPower has installed a 35-kV class saturated cores FCL in China Southern Power Grid [1] and moved on in 2012 to develop a 220-kV class saturated cores FCL [2]. Zenergy Power has installed in 2009 a 12-kV saturated cores FCL at the Southern California Edison Grid [3]. Recently, GridON has installed an 11 kV class saturated cores FCL at a UK Power Network substation in Newhaven [4]. A larger 11-kV class FCL by GridON is being commissioned for a substation at Birmingham, UK, at the Western Power Distribution Grid [5].

The worldwide effort towards an industrial FCL device requires deep understanding of the saturated cores FCL behavior. In principle, the saturated cores FCL is a device placed in series in the grid, which passively and automatically changes its impedance from low-impedance state at normal grid operation to high-impedance state during a fault. As described already in the 1980s in a series of papers by Parton et al. [6], this is achieved by applying a DC bias field to saturate magnetic cores on which the AC grid coils are mounted. The superposition of the DC and opposing AC magnetic flux in the core determines the core state and the AC coil impedance. When the AC flux is small in comparison with the DC flux, the core is saturated and the impedance is low (normal state). When the AC flux becomes comparable to the DC flux, the core is desaturated and the impedance increases (fault state).

Two of the saturated cores FCL's main characteristics are its normal and fault state impedances. Traditionally, the dimensions of the saturated cores FCL are derived from the fault state impedance using a simplified relation:

$$X_{\text{fault}} \approx \frac{V_p}{\sqrt{2} I_{\text{fault}}} \approx \frac{4\pi f N A_{\text{core}} B_{\text{sat}}}{\sqrt{2} I_{\text{fault}}} \quad (1)$$

Y. Nikulshin · Y. Wolfus (✉) · A. Friedman · Y. Yeshurun
Department of Physics, Institute of Superconductivity and Institute of Nanotechnology and Advanced Materials, Bar-Ilan University, 5290002 Ramat-Gan, Israel
e-mail: shuki.wolfus@gmail.com

where X_{fault} is the fault state impedance, V_p is the peak voltage, f is grid frequency, N is the number of turns in the AC coil, A_{core} is the crosssection of the core, B_{sat} is the saturation induction and I_{fault} is the limited root mean square fault current. Such relations between the fault impedance and the FCL's dimensions were used in many works [7–9], and the fault and normal impedances are often used to characterize the FCL. While these impedance values provide some information about the saturated cores FCL and its dimensions, most of the information about the operation of the FCL remains concealed. We claim that the dynamics of the transition between the saturated and desaturated core states, which is often ignored, provide deeper insight into the operation of the saturated cores FCL and may be used to design more efficient devices with smaller dimensions. In this work, we study the dynamic inductance in a saturated cores FCL configuration example and show its important contribution to the device limiting performances.

2 Experimental

Figure 1 exhibits the saturated cores FCL model studied in this work. This design uses single magnetic core. Two bias DC coils are mounted on the short limbs of the magnetic core and form a closed DC magnetic circuit. The AC coils are connected in series and mounted on the long limbs generating magnetic flux in the same direction, hence forming an open AC magnetic circuit. In addition, the orthogonal DC and AC coils ensure minimal transformer coupling between them. The FCL, with the parameters listed in Table 1, was connected to the laboratory AC 230 V, 50 Hz power. The two major advantages of this configuration compared to other saturated cores FCL configurations are: dramatically reduced AC-DC coupling and single core usage for both AC half cycles.

Measurements of the FCL characteristics have been performed both experimentally, by measuring current and voltage across the coils, and by finite element method (FEM) simulations. Cobham Vector Fields was used for calculating magnetic induction and flux distribution in the cores and for calculating coil inductances. MATLAB was used to solve numerically the equations below, given the parameters extracted from measurements and simulations.

Table 1 Parameters of the saturated cores FCL model

FCL element	Parameter	Value
Core	AC leg length, mm	300
	AC leg cross-section, mm	40 × 40
	DC leg cross-section, mm	50 × 40
AC coil	Length, mm	200
	Number of turns	148
DC coil	Number of turns	200

3 Results and Discussion

Since laminated transformer steel is used for the core material, in the following calculations magnetic hysteresis is neglected. Therefore, the differential equation describing the voltage in a grid that includes saturated cores FCL is

$$V\cos(\omega t) = I\left(R_{load}+R_{grid}+R_{fcl}\right)+L_{grid}\frac{dI}{dt}+\frac{d}{dt}(LI) \tag{2}$$

where L_{grid} and R_{grid} are inductance and resistance of the circuit elements, R_{load} is the load resistance, and I is the current. The saturated cores FCL inductance, L, depends on the core magnetic state. The lower limit for L is defined by air inductance of the coil and obtained when the core is deeply saturated by the DC bias coils. In this state, the relative permeability approaches one. The increase of AC current through the FCL drives the core out of saturation causing the relative permeability to increase; hence, L increases with increasing current. The upper limit of L is obtained for a current value where the average relative permeability across the coil is maximal. Further increase of AC current drives the core into reversed saturation and L decreases correspondingly. Therefore, the current dependence of L is nonlinear and non-monotonic, leading to the unique FCL behavior discussed below.

The shape of the $L(I)$ curve plays an important role in determining the voltage drop across the FCL terminals. This voltage is described by the following:

$$\begin{aligned} V_{fcl} &= IR_{fcl}+N\frac{d\Phi}{dt} = IR_{fcl}+\frac{d}{dt}(LI) \\ &= IR_{fcl}+L_{fcl}\frac{dI}{dt}+I\frac{dL_{fcl}}{dt} \end{aligned} \tag{3}$$

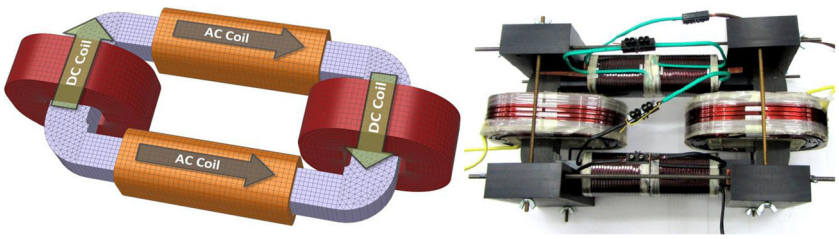

Fig. 1 3D model of the single-phase saturated cores FCL model. *Right*: Actual model studied

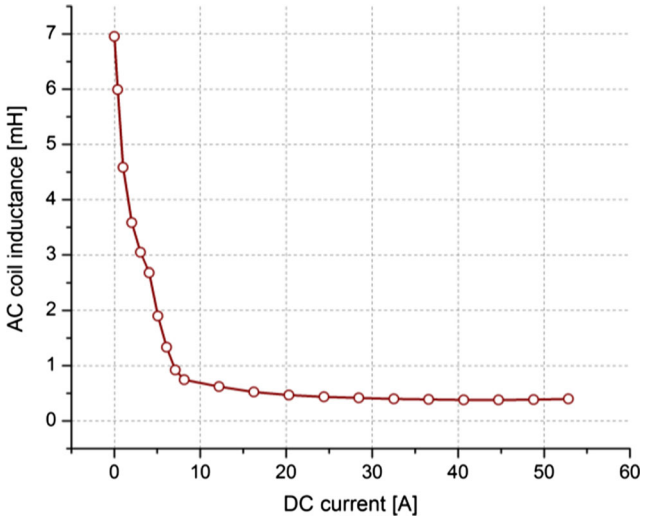

Fig. 2 Dependence of the inductance of one AC coil on the DC bias level

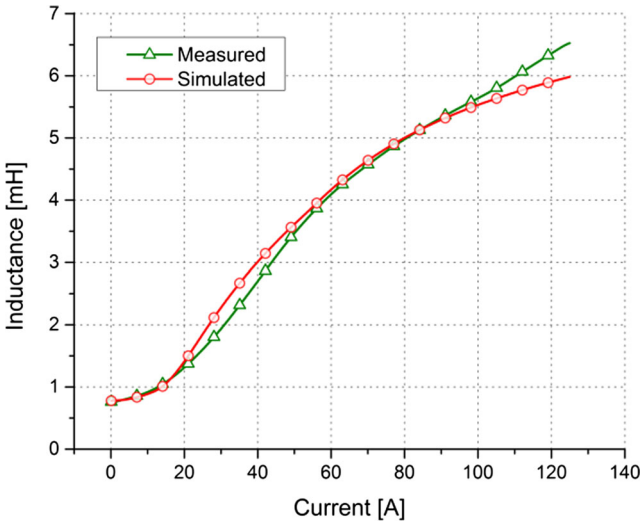

Fig. 4 Calculated $L(I)$ curves from measurement data (*green*) and simulated data (*red*)

If the function $L(I)$ is known, (2) and (3) can be solved analytically and the full system performance can be calculated. This includes the exact $V(t)$ and $I(t)$ waveforms at any point in the grid. When $L(I)$ is obtained experimentally, these equations can still be solved numerically. Such numerical solutions provide a comprehensive description of the FCL performance at any given state.

To derive $L(I)$ experimentally, measurements of the AC coil inductance were done while applying current in the bias coils ranging from 0 to 52.5 A. At every step, the AC coil inductance was measured by applying a small AC current in the AC coils. To ensure the core magnetization does not change much by the AC current, it was kept at least 4 orders of magnitudes smaller than the DC current.

Figure 2 exhibits the dependence of L measured on one of the AC coils as a function of the DC bias current. A sharp decrease in L is observed at currents up to about 8 A. Further increase of bias current drives the core into saturation state, and L gradually approaches 0.34 mH, the air-core inductance of the AC coil.

Once a DC bias current is selected, the current dependent inductance $L(I)$ during an AC current cycle can be retrieved. In the case presented here, DC current of 43 A in each coil (equivalent to 8,600-A turns) was used. It is important to note that for each DC bias current, different $L(I)$ curve is obtained and determines the FCL operation. To obtain the $L(I)$ curve, the current in the AC coils was ramped and the voltage across both AC coils was measured.

In the above procedure, one optimizes an existing saturated cores FCL device. To enable optimization of the FCL already during the design process (i.e., the device does not yet exist), we have also evaluated the $L(I)$ curve by using transient FEM simulations. The 3D FCL model used for the simulations has the same geometry and parameters as the experimental model (Fig. 1, Table 1). It is important to note that thermal simulations of the core are omitted in

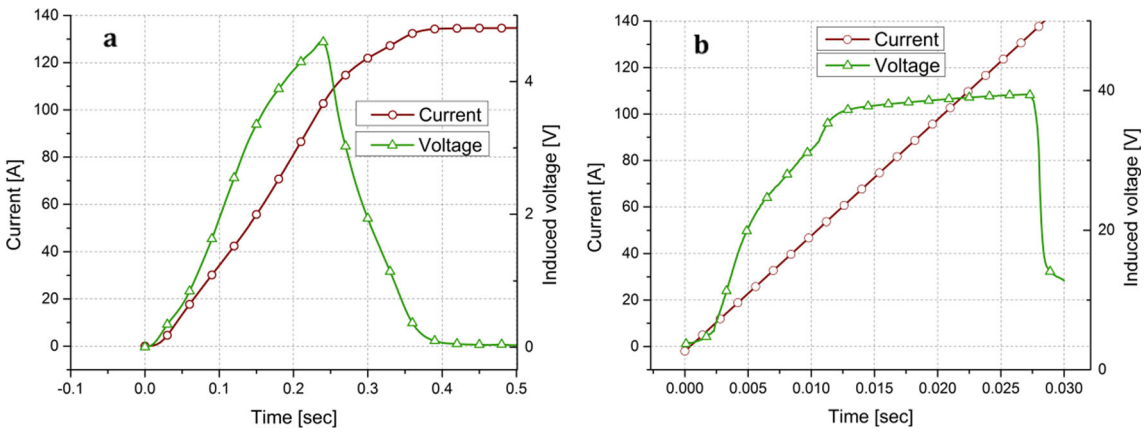

Fig. 3 Current ramp (*red*) and induced voltage (*green*) across an AC coils. **a** Physical measurement **b** FEM simulation

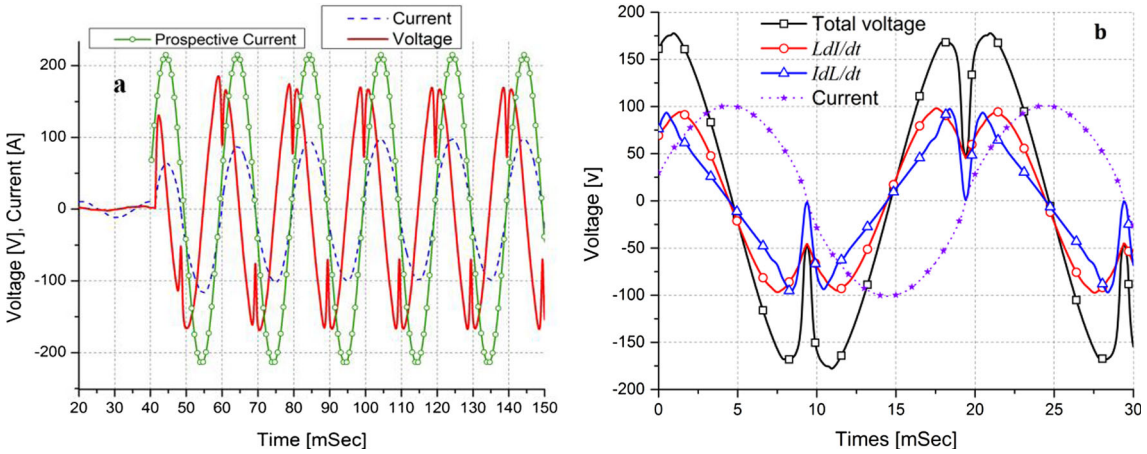

Fig. 5 **a** Measured waveforms of the FCL voltage, current, and prospective current. **b** Calculated contributions of the FCL voltage components

this treatment. This is justified because the core is made of laminated transformer sheets so that eddy currents are minimized. Also, during normal FCL operation, deeply saturated and hysteresis losses may be neglected.

Given the current and voltage time dependent curve of Fig. 3, $L(I)$ was then calculated by numerically integrating over (3):

$$L(I,t) = \frac{\int \left(V_{fcl} - IR_{fcl}\right) dt}{I_{(t)}} \tag{4}$$

Figure 4 exhibits the $L(I)$ curves obtained by this procedure. The nice agreement between the measured and simulated curves suggest that this procedure for obtaining $L(I)$ of an FCL device may serve as an important design tool and save precious time and resources

After obtaining the $L(I)$ curve of the FCL, one may go back to (3) and obtain the full behavior of the FCL in the grid for any given current waveform. To demonstrate the strength of this method, we present in Fig. 5a the current and voltage curves during a fault event. Figure 5b zooms on one cycle of the fault current and describes the contribution of each of the inductive components in (3). Clearly, the component *IdL/dt* adds a significant contribution to the total voltage drop on the FCL. In particular, at low currents where the absolute value of L is still low but the rate of change in $L(I)$ is high, this contribution overcomes the contribution by the traditional term *LdI/dt*. This result suggests that the dynamic inductance component cannot be overlooked and should be examined when designing a saturated cores FCL

4 Summary

A method for extracting the nonlinear $L(I)$ curves of saturated cores FCLs has been developed. This method may be applied as a tool for optimizing the saturated cores FCL design and performances. Given the $L(I)$ curve, the full voltage drop across the saturated cores FCL at any state is calculated and shows that the dynamic inductance term *IdL/dt* contributes significantly to the total voltage drop and dominates over the static inductance term at some portions of the AC current cycle. The dynamic inductance term should not be neglected in designing a saturated cores FCL model, and it may be used for reducing the core cross-section and the overall device dimensions required when this term is neglected.

Acknowledgments This work was supported in part by the Israeli Ministry of Energy and Water.

References

1. Xin, Y., Wang, J.Z., Hong, H., Gong, W.Z., Zhang, J.Y., Niu, X.Y., Ren, a.L., Si, D.J., Zi, M.R., Xiong, Z.Q., Ye, F.: Field tests on a 35kV/90MVA superconducting fault current limiter. 2010 Int. Conf. Power Syst. Technol., 1–5 (2010)
2. Xiao, H., Qiu, J., Wang, S., Zhang, Q., Gong, W., Xin, Y., Zhu, J.G., Guo, Y.: Analysis of transient overvoltage in 220 kV saturated core HTS FCL. IEEE Trans. Magn. **47**, 2620–2623 (2011)
3. Moriconi, F., De La Rosa, F., Darmann, F., Nelson, A., Masur, L.: Development and deployment of saturated-core fault current limiters in distribution and transmission substations. IEEE Trans. Appl. Supercond. **21**, 1288–1293 (2011)
4. GridON's Fault Current Limiter commissioned into service by ETI at a UK Power Networks substation, http://www.eti.co.uk/news/article/gridons_fault_current_limiter_commissioned_into_service_by_eti_at_a_uk_powe
5. GridON: GridON signed contract to supply a 30MVA Fault Current Limiter to Western Power Distribution for a primary substation in Birmingham, UK. (2014). http://gridon.com/news_events.html#WPDcontract

6. Raju, B., Parton, K., Bartram, T.: A current limiting device using superconducting D.C. Bias Applications and Prospects. IEEE Trans. Power Appar. Syst. PAS-101, 3173–3177 (1982)
7. Cvoric, D., Haan, S.: De: Design and testing of full-scale 10 kV prototype of inductive fault current limiter with a common core and trifilar windings. Syst. (ICEMS) (2010)
8. Moscrop, J., Darmann, F.: Design and development of a 3-phase saturated core high temperature superconducting fault current limiter. Electr. Power Energy Convers. (2009)
9. Zong, X.H., Wang, J.X., Sun, J., Wang, Y.N.: Study on inductive high-T_c superconducting fault current limiters. Phys. C Supercond. **386**, 522–526 (2003)